

Information-Theoretic Signatures of Biodiversity in the Barcoding Gene

Valmir C. Barbosa*

Programa de Engenharia de Sistemas e Computação, COPPE
Universidade Federal do Rio de Janeiro
Caixa Postal 68511
21941-972 Rio de Janeiro - RJ, Brazil

Abstract

The COI mitochondrial gene is present in all animal phyla and in a few others, and is the leading candidate for species identification through DNA barcoding. Calculating a generalized form of total correlation on publicly available data on the gene yields distinctive information-theoretic descriptors of the phyla represented in the data. Moreover, performing principal component analysis on standardized versions of these descriptors reveals a strong correlation between the first principal component and the natural logarithm of the number of known living species. The descriptors thus constitute clear information-theoretic signatures of the processes whereby evolution has given rise to current biodiversity.

Keywords: Information content of DNA, COI mitochondrial gene, Folmer region.

*valmir@cos.ufrj.br

1 Introduction

The genome of every living organism is the product of Darwinian natural selection and random drift as they played out along the ages since the inception of life on the planet. The fundamental hallmark of this lengthy process has been the appearance and diversification of highly organized (out of highly unorganized) matter. It is therefore only expected that any pool of DNA from a sufficiently representative set of individuals should contain unmistakable information-theoretic traces of how the reduction of entropy that the evolution of life has entailed led to the biodiversity that we observe today. This notwithstanding, previous efforts to analyze the information content of DNA have been limited in scope and as such provided little or no insight into biodiversity [1–4].

As we see it, there are two main difficulties to be faced when attempting such analyses. The first one has to do with the availability of experimental data, as well as with the quality of such data when they are available. Any information-theoretic analysis of DNA has to begin by grappling with estimating the distribution of probability associated with the pool that is being studied. If the pool comes, say, from a single genus, and given some individual of that genus, we must be able to estimate the probability that the genus contains DNA that is sufficiently similar to that observed for the given individual. Moreover, this only makes sense if the DNA in question comes from a region of the genome that is found in all individuals in that genus, which further complicates the data availability and quality problem. The second difficulty has to do with formulating the problem adequately. While the well-known Shannon entropy can be effectively used to quantify information gain, it needs to be applied carefully in order to tease out the desired footprints of biodiversity.

Here we address the first difficulty by taking advantage of the current public availability of data on the so-called barcoding gene (the COI mitochondrial gene) from the BOLD (Barcode Of Life Data) systems initiative [5]. This gene is present in all animals as well as in members of a few other phyla [6]. The BOLD repository contains a few million sequence fragments of the gene’s 710-base-pair Folmer region [7], covering 25 phyla, of which 23 are animal phyla and the remaining two are phyla of algae. The barcoding gene is therefore ubiquitous to a large extent. It is also diverse enough across species (thence its denomination as a “barcode” [8]), so the BOLD samples are poised to constitute a suitable dataset from which to estimate the necessary probability distributions. Owing to the way in which these data are organized, we perform our study at the level of the phylum.

As for the difficulty of formulating the problem adequately, we follow the principle first expressed qualitatively by Rothstein in 1952 regarding the analysis of information gain in the multivariate case [9]. This principle considers a set of random variables representing some physical process of interest, as well as their joint distribution. It states that, since information gain occurs during the process not only at the level of the set of all variables taken as a whole but also at the level of any of its subsets, what really matters is the amount of global gain that surpasses the combined local gains relative to select subsets. This

principle has been formalized as the so-called total correlation of the variables and its generalizations [10]. It is behind several studies related to the integration of information in complex systems, including some targeted at the temporal evolution of probabilistic cellular automata [11], of threshold-based systems in general [12], and of the cerebral cortex as it gives rise to consciousness [13–15].

We use a particular form of generalized total correlation to obtain information-theoretic descriptors of the barcoding gene for each of the phyla considered. These descriptors are correlated with one another to various degrees, but mapping them onto the uncorrelated, variance-emphasizing directions provided by PCA (principal component analysis) [16] reveals them to be signatures of biodiversity that lie hidden in the gene. Specifically, for each phylum a single new descriptor is obtained that correlates strongly with the biodiversity that is present in the phylum as expressed by the logarithm of its number of species (either those represented in the data or the many more that are known but have not yet reached the BOLD system). Biodiversity, therefore, is seen to grow exponentially with that single descriptor of a phylum.

2 Generalized total correlation

Let $S = \langle S_1, S_2, \dots, S_n \rangle$ be an n -nucleotide sequence, i.e., each S_k is one of the four nucleotides occurring in DNA (represented by base A, C, G, or T), and let \mathcal{B}_n be the set of all 4^n n -nucleotide sequences. We assume that n is a multiple of 3 (the number of nucleotides in a codon) and view each S_k as a random variable. The form of generalized total correlation that we use is based on partitioning S into contiguous subsequences. The number of possible partitions is exponential in n , which probably would rule out any attempt at choosing an optimal one given the ultimate goal of exposing biodiversity even if such optimality were well defined. The partition we select requires every subsequence to be $d < n$ nucleotides long, with n a multiple of d and d a multiple of 3. The number of subsequences in the partition is n/d .

Our version of generalized total correlation is specific to sequence S of random variables and divisor d . It is denoted by $C(S, d)$ and given by the Kullback-Leibler divergence from the joint distribution of the n random variables that would ensue if all n/d subsequences were probabilistically independent of one another to the actual joint distribution. That is,

$$C(S, d) = \sum_{T \in \mathcal{B}_n} \Pr(S = T) \log_4 \frac{\Pr(S = T)}{\prod_{i=1}^{n/d} \Pr(S_{id-d+1}^{id} = T_{id-d+1}^{id})}, \quad (1)$$

where each S_k^ℓ , with $\ell - k + 1 = d$, denotes the d -nucleotide sequence beginning at nucleotide S_k and ending at nucleotide S_ℓ , and similarly for T_k^ℓ . This expression can be rewritten as

$$C(S, d) = \sum_{i=1}^{n/d} H(S_{id-d+1}^{id}) - H(S), \quad (2)$$

where

$$H(S_k^\ell) = - \sum_{T \in \mathcal{B}_d} \Pr(S_k^\ell = T_k^\ell) \log_4 \Pr(S_k^\ell = T_k^\ell) \quad (3)$$

and

$$H(S) = - \sum_{T \in \mathcal{B}_n} \Pr(S = T) \log_4 \Pr(S = T) \quad (4)$$

give the Shannon entropy of S_k^ℓ and that of S , respectively (\mathcal{B}_d is the set of all 4^d d -nucleotide sequences). The use of logarithms to the base 4 implies $H(S_k^\ell) \leq d$ for each pair k, ℓ and $H(S) \leq n$. These bounds, in turn, suggest a reinterpretation of Eq. (2), after rewriting it in the form

$$C(S, d) = [n - H(S)] - \sum_{i=1}^{n/d} [d - H(S_{id-d+1}^{id})], \quad (5)$$

where each term in square brackets is an information gain, or reduction of entropy, relative to the case of maximum entropy. The reinterpretation, therefore, is of $C(S, d)$ as the amount of global information gain (i.e., relative to sequence S) that surpasses the sum total of the local information gains (i.e., relative to the subsequences S_k^ℓ). $C(S, d)$ is expressed in quaternary digits (*quats*), but henceforth we use its normalized version, denoted by $N(S, d)$ and given by

$$N(S, d) = \frac{C(S, d)}{n - d}, \quad (6)$$

whose denominator gives the maximum possible value of $C(S, d)$.

3 Methods

All data publicly available at the BOLD website (barcodinglife.org) on September 20, 2017 were downloaded in the FASTA format. All sequences start at the 5'-end of the barcoding gene but not all have the same number of nucleotides. Moreover, sequences often contain symbols other than A, C, G, or T, following the FASTA convention that hyphens and other eleven letters can also appear and have specific meanings: a hyphen denotes a gap of indeterminate length produced during sequencing; the other letters indicate uncertainty in tagging the signal that is read off the sequencer with one of the four base letters (for example, R indicates uncertainty between A and G; B indicates uncertainty among the non-A bases; and N indicates full uncertainty).

In order to allow each available sequence to contribute as fully as possible, each one can give rise to several others, each of a different length. This is achieved by truncating the original sequence to its first 432 nucleotides, then to the first 459 nucleotides, then 486, and so on through 702 nucleotides. Depending on how each of these numbers relates to the original length, each sequence can yield anywhere from none up to eleven sequences for use in the study, possibly including one with the 648 nucleotides of the canonical barcoding gene fragment [5].

Before participating in the estimation of the joint distribution, each sequence thus generated is screened and discarded if either of two flags is raised. The first one indicates the presence of a hyphen. The second indicates the presence of too many letters other than A, C, G, or T. In order to decide whether to raise this second flag, we first assign an unfolding factor to each letter in the sequence. The factor assigned to the k th letter is $q_k = 1$ if the letter is A, C, G, or T; $q_k = 2$ if the letter expresses uncertainty between two of those four (such as R, used above in the example); $q_k = 3$ if the uncertainty is among three of them (such as B in the example); or $q_k = 4$ if the letter is N. The flag is raised if $Q > 1000$, where $Q = \prod_{k=1}^n q_k$, which is meant to ensure that the storage required for computing does not run out of bounds during distribution estimation.

The number of surviving sequences for each phylum and for each of $n = 432, 459, \dots, 702$ is shown in Table A.1. This has led to the elimination of two phyla from the study, Cyclophora and Gnathostomulida, due to the absence, for at least one value of n , of surviving sequences. We therefore proceed with a total of 23 phyla. For each of these phyla, the total number of $N(S, d)$ descriptors is 107, all eleven values of n considered, every multiple-of-3 divisor d of each n considered as well (except for n itself).

For each phylum and each value of n , the essential probability to be estimated is the joint probability $\Pr(S = T)$ for each $T \in \mathcal{B}_n$, since from these all marginals related to the subsequences of S can be computed. A first approach to such estimation, the so-called plug-in approach, is to first count the number of occurrences of T among the sequences that survived screening and then normalize the counts. Because \mathcal{B}_n only contains sequences of the base letters A, C, G, and T, each surviving sequence is first unfolded into Q sequences that only have base letters as well. Each of these Q sequences includes one full set of the possible replacements of the non-base letters with base letters that resolve the uncertainties, and receives a contribution of $1/Q$ to its count.

This approach sets $\Pr(S = T)$ to 0 for nearly all $T \in \mathcal{B}_n$, which can sometimes be too imprecise due to the limited number of surviving sequences (even after unfolding). There would be nothing else to be done if distribution estimation were the final goal, but for entropy calculations from the estimated distribution there are several approaches that seek to alleviate the problem [17–19]. In this study we use the Hausser-Strimmer shrinkage approach [18], which essentially begins with the same counting as above and then alters the resulting probabilities via a data-dependent convex combination with the uniform distribution over \mathcal{B}_n .

A crucial methodological ingredient is to drastically simplify the description of each phylum as a point in 107 dimensions to one in only a few dimensions. We do this by viewing each of the 107 $N(S, d)$ descriptors as a random variable for which 23 samples are available (one for each phylum) and using PCA on these variables’ standardized versions (obtained by shifting and scaling each variable’s samples so that the resulting mean and standard deviation are 0 and 1, respectively). PCA returns a description of the phyla in terms of principal components, that is, uncorrelated projections of the random variables’ standard-

ized samples. The first component accounts for more variance across the phyla than the second, the second more than the third, and so on. One then retains as many of these components as needed to account for as much variance as desired, hopefully only a few of them. Projecting a phylum’s 107-dimensional vector of standardized samples onto one of the retained components is achieved by a zero-intercept linear regression through the 107 coefficients that PCA outputs, known as that component’s loadings.

4 Results

For each of the 23 phyla whose BOLD data survived screening we obtained all 107 $N(S, d)$ descriptors as outlined. Drawing a scatter plot for each phylum with each descriptor represented by its d/n and $N(S, d)$ values yields a rich variety of possibilities, as illustrated in Figure A.1 for all phyla and in Figure 1 for Arthropoda and Porifera. These two phyla were singled out because they illustrate particularly well how striking the difference between the descriptors of distinct phyla can be. In fact, even though for any given phylum the value of $N(S, d)$ decreases with increasing d for fixed n [note that the unnormalized value of $N(S, d)$, $C(S, d)$, equals 0 for $d = n$, regardless of the underlying joint distribution], visually it is clear that sometimes the descriptors of two given phyla share not much else.

Applying PCA yields a first principal component that accounts for 90.36% of the variance across the phyla, a second component accounting for 5.67% of such variance, and so on, as shown in the so-called scree plot of Figure A.2. Projecting the 107-dimensional standardized phylum samples onto the first two principal components yields the scatter plot shown in Figure 2, where therefore over 96% of the variance is accounted for. The first principal component, in particular, suggests a nearly unique ordering of the phyla, from the ones with the most negative values (Priapulida and Xenoturbellida) to the one with the most positive value (Arthropoda). This order is used in Table 1 to list all phyla along with two numbers of species for each phylum. The first one (N.Sp.) is the number of species accounted for in the data for that phylum and the second (N.Liv.Sp.) is the number of known living species the phylum has. N.Sp. is a lower bound on the number of species represented in the data, since not all sequences are tagged with a species name. Note that, regardless of which species count one focuses on, there is a general tendency for the number of species to grow rapidly as the phyla are considered in the order of increasing first principal component.

In fact, computing the Pearson correlation coefficient between the first principal component and the natural logarithm of the number of species over all 23 phyla yields a little over 0.96 for N.Sp., a little over 0.93 for N.Liv.Sp. The corresponding linear models are given in Figure 3. We find it a striking feature of these models that, in both cases, their slopes are practically the same: 0.28535 and 0.28680, respectively for N.Sp. and N.Liv.Sp., the latter only 0.5% above the former. Thus, not only are the $N(S, d)$ descriptors strong information-theoretic

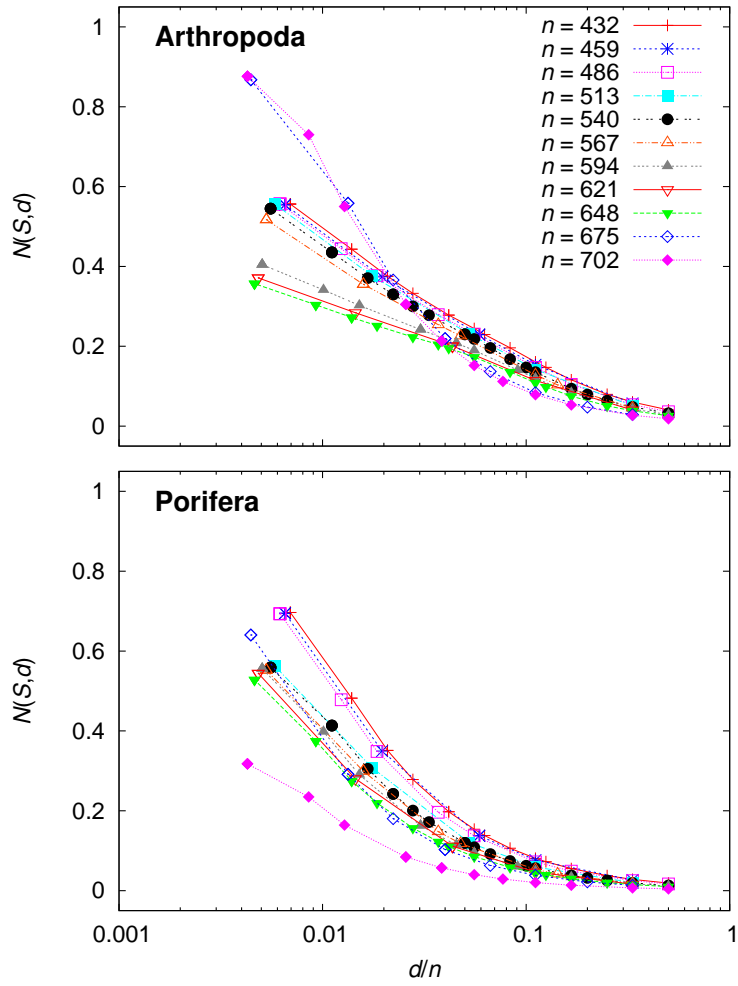


Figure 1: The 107 $N(S, d)$ descriptors for the phyla Arthropoda and Porifera.

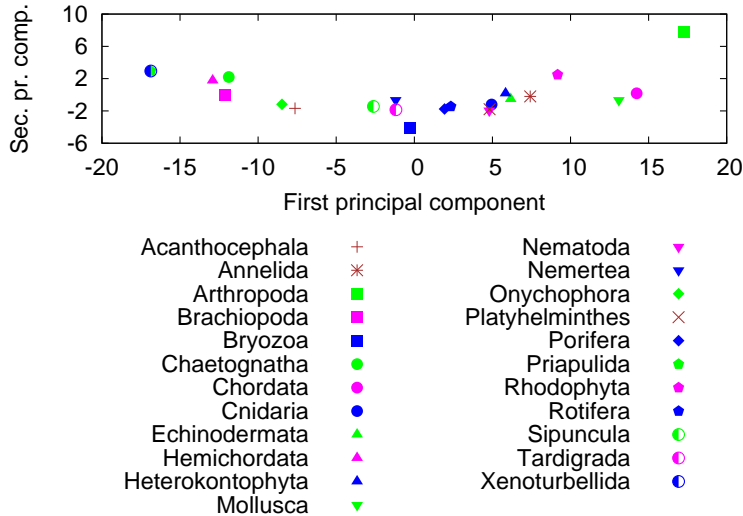


Figure 2: Each phylum as represented by the first and second principal components of all 107 standardized $N(S, d)$ descriptors. The symbol for Priapulida is covered by that for Xenoturbellida.

signatures of a phylum’s biodiversity as annotated in the available data on the barcoding gene, they are also seen to be robust signatures, since they relate nearly as significantly to all the known biodiversity that is mostly absent from the data.

5 Conclusion and outlook

The discovery related in this paper has been driven mainly by data, following an initial intuition regarding the nature of information gain as expressed by the generalized forms of total correlation, as well as the primacy of the codon, rather than the nucleotide, as the most meaningful structural unit. While this data-centric approach may seem only natural in an age of successful machine learning and data science in general, we believe such discoveries beg many more questions than they answer. In the case at hand, a principled theory supporting what has been discovered is still lacking and should be pursued. One necessary first step toward further understanding is to interpret the loadings of the first principal component. These are shown in Figure 4, where we see that loadings are less influential for the largest values of n . Likewise, for $n \leq 648$ they peak at around $d = 27\text{--}54$ nucleotides, that is, 9–18 codons.

Moreover, our claim that the $N(S, d)$ descriptors constitute robust signatures of biodiversity (since they lead to essentially same-slope linear models regardless of whether the number of species in question is that taken from the data or

Table 1: Lower bound on the number of species represented in the data (N.Sp.), as reported on the BOLD website (barcodinglife.org) on September 20, 2017; and number of known living species (N.Liv.Sp.), as reported on the Encyclopedia of Life website (eol.org/collections/18879) on November 1, 2017 (two exceptions are the N.Liv.Sp. values for Heterokontophyta and Rhodophyta, obtained from wikipedia.org/wiki/Heterokont and wikipedia.org/wiki/Red_algae, respectively, on October 21, 2017). Phyla are listed in the order of increasing first principal component, as implied by Figure 2. A tie exists between Priapulida and Xenoturbellida, which are then listed in the order of increasing N.Sp. (or N.Liv.Sp.).

Phylum	N.Sp.	N.Liv.Sp.
Xenoturbellida	1	2
Priapulida	2	19
Hemichordata	2	120
Brachiopoda	35	443
Chaetognatha	30	179
Onychophora	90	179
Acanthocephala	36	1 192
Sipuncula	64	144
Nemertea	172	1 200
Tardigrada	67	1 157
Bryozoa	163	5 486
Porifera	656	8 346
Rotifera	289	1 583
Nematoda	521	24 773
Platyhelminthes	729	29 285
Cnidaria	1 702	10 105
Heterokontophyta	465	25 000
Echinodermata	1 278	7 509
Annelida	2 400	17 446
Rhodophyta	2 659	7 000
Mollusca	9 768	117 358
Chordata	21 035	64 791
Arthropoda	132 834	1 235 858

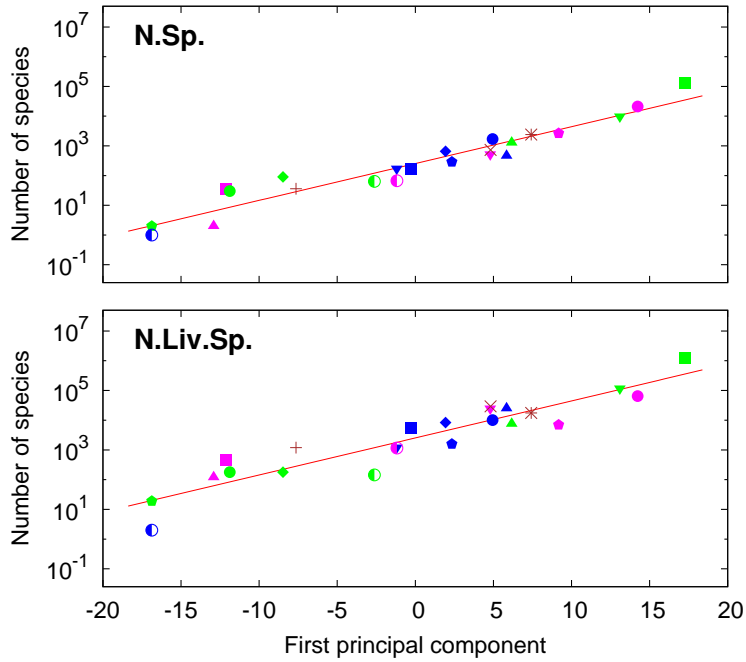


Figure 3: Each phylum as represented by the first principal component of all 107 standardized $N(S, d)$ descriptors and by the number of species in the phylum (either the lower bound given by the data, N.Sp., or the number of known living species, N.Liv.Sp.; see Table 1). The fitted linear models for N.Sp. and N.Liv.Sp. are $\ln y = 5.53792 + 0.28535x$ (p-value: 2.256×10^{-12}) and $\ln y = 7.83349 + 0.28680x$ (p-value: 7.982×10^{-11}), respectively. Symbol keys are the same as in Figure 2.

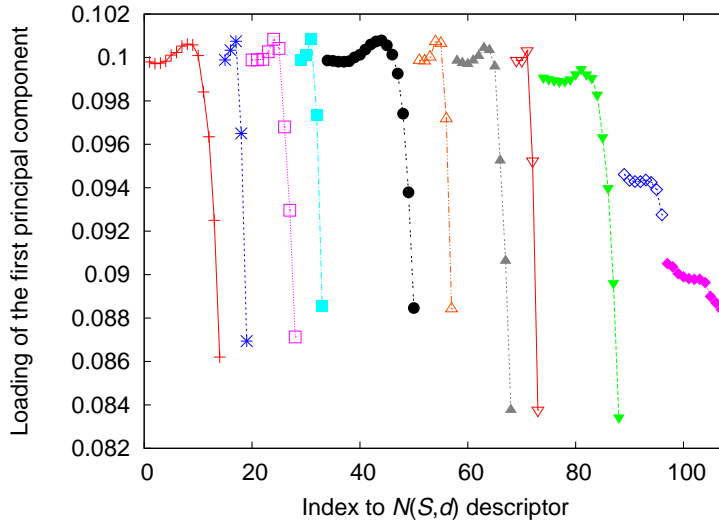


Figure 4: Loadings of the first principal component for each of the 107 standardized $N(S, d)$ descriptors. Descriptors are indexed upward from 1, arranged lexicographically on the pair n, d . Symbol keys are the same as in Figure 1.

that of the known living species) should stand in the face of further scrutiny. In this regard, not only does the BOLD repository tend to grow continually, but perhaps more importantly, most biodiversity and conservation specialists seem convinced that the number of undiscovered living species surpasses that of known living species by a wide margin [20–22]. Robustness is then to be reevaluated whenever the availability of data or the number of known living species gets substantially modified.

Acknowledgments

We acknowledge partial support from CNPq, CAPES, and a FAPERJ BBP grant.

References

- [1] L. L. Gatlin. The information content of DNA. *J. Theor. Biol.*, 10:281–300, 1966.
- [2] R. H. Crozier. Preserving the information content of species: genetic diversity, phylogeny, and conservation worth. *Annu. Rev. Ecol. Syst.*, 28:243–268, 1997.
- [3] A. O. Schmitt and H. Herzel. Estimating the entropy of DNA sequences. *J. Theor. Biol.*, 188:369–377, 1997.

- [4] S. Srivastava and M. S. Baptista. Markovian language model of the DNA and its information content. *Roy. Soc. Open Sci.*, 3:150527, 2016.
- [5] S. Ratnasingham and P. D. N. Hebert. BOLD: the barcode of life data system (www.barcodinglife.org). *Mol. Ecol. Notes*, 7:355–364, 2007.
- [6] P. D. N. Hebert, A. Cywinska, S. L. Ball, and J. R. deWaard. Biological identifications through DNA barcodes. *Proc. R. Soc. Lond. B*, 270:313–321, 2003.
- [7] O. Folmer, M. Black, W. Hoeh, R. Lutz, and R. Vrijenhoek. DNA primers for amplification of mitochondrial cytochrome *c* oxidase subunit I from diverse metazoan invertebrates. *Mol. Mar. Biol. Biotech.*, 3:294–299, 1994.
- [8] V. Savolainen, R. S. Cowan, A. P. Vogler, G. K. Roderick, and R. Lane. Towards writing the encyclopaedia of life: an introduction to DNA barcoding. *Phil. Trans. R. Soc. B*, 360:1805–1811, 2005.
- [9] J. Rothstein. Organization and entropy. *J. Appl. Phys.*, 23:1281–1282, 1952.
- [10] S. Watanabe. Information theoretical analysis of multivariate correlation. *IBM J. Res. Dev.*, 4:66–82, 1960.
- [11] K. K. Cassiano and V. C. Barbosa. Information integration in elementary cellular automata. *J. Cell. Autom.*, 10:235–260, 2015.
- [12] V. C. Barbosa. Information integration from distributed threshold-based interactions. *Complexity*, 2017:7046359, 2017.
- [13] D. Balduzzi and G. Tononi. Integrated information in discrete dynamical systems: motivation and theoretical framework. *PLoS Comput. Biol.*, 4:e1000091, 2008.
- [14] A. Nathan and V. C. Barbosa. Network algorithmics and the emergence of information integration in cortical models. *Phys. Rev. E*, 84:011904, 2011.
- [15] M. Oizumi, L. Albantakis, and G. Tononi. From the phenomenology to the mechanisms of consciousness: integrated information theory 3.0. *PLoS Comput. Biol.*, 10:e1003588, 2014.
- [16] H. Abdi and L. J. Williams. Principal component analysis. *WIREs Comput. Stat.*, 2:433–459, 2010.
- [17] L. Paninski. Estimation of entropy and mutual information. *Neural Comput.*, 15:1191–1253, 2003.
- [18] J. Hausser and K. Strimmer. Entropy inference and the James-Stein estimator, with application to nonlinear gene association networks. *J. Mach. Learn. Res.*, 10:1469–1484, 2009.

- [19] E. Archer, I. M. Park, and J. W. Pillow. Bayesian entropy estimation for countable discrete distributions. *J. Mach. Learn. Res.*, 15:2833–2868, 2014.
- [20] C. Mora, D. P. Tittensor, S. Adl, A. G. B. Simpson, and B. Worm. How many species are there on Earth and in the ocean? *PLoS Biol.*, 9:e1001127, 2011.
- [21] B. R. Scheffers, L. N. Joppa, S. L. Pimm, and W. F. Laurance. What we know and don't know about Earth's missing biodiversity. *Trends Ecol. Evol.*, 27:501–510, 2012.
- [22] B. R. Larsen, E. C. Miller, M. K. Rhodes, and J. J. Wiens. Inordinate fondness multiplied and redistributed: the number of species on Earth and the new pie of life. *Q. Rev. Biol.*, 92:229–265, 2017.

A Supplementary material

This appendix collects Table A.1 and Figures A.1 and A.2.

Table A.1: Number of sequences downloaded (N.D.) and resulting from screening for each value of n .

Phylum	N.D.	$n = 432$	$n = 459$	$n = 486$	$n = 513$	$n = 540$
Acanthocephala	465	341	243	243	242	239
Annelida	31 700	22 931	22 850	22 658	22 048	21 581
Arthropoda	3 854 064	3 054 118	3 040 943	3 005 920	2 987 772	2 884 779
Brachiopoda	85	12	12	12	12	12
Bryozoa	1 611	1 303	1 126	1 028	897	894
Chaetognatha	287	185	185	132	132	131
Chordata	304 239	250 169	249 322	247 814	246 555	243 226
Cnidaria	9 593	6 667	6 374	6 181	6 051	5 824
Cycliophora	273	31	31	31	0	0
Echinodermata	19 939	13 080	13 072	12 890	12 662	12 549
Gnathostomulida	8	0	0	0	0	0
Hemichordata	12	10	10	10	10	10
Heterokontophyta	4 366	4 263	4 207	4 200	4 059	4 056
Mollusca	99 413	61 792	60 719	59 988	58 305	55 758
Nematoda	4 894	3 133	2 637	2 632	2 625	2 544
Nemertea	942	613	612	612	607	593
Onychophora	658	450	379	379	379	354
Platyhelminthes	8 297	5 609	5 346	3 917	3 837	3 748
Porifera	2 133	1 654	1 638	1 625	1 326	1 292
Priapulida	4	3	3	3	3	3
Rhodophyta	29 703	21 121	21 082	20 759	20 730	20 659
Rotifera	6 261	4 995	4 968	4 899	3 819	3 742
Sipuncula	363	299	298	298	298	298
Tardigrada	729	700	694	692	653	605
Xenoturbellida	2	1	1	1	1	1
	$n = 567$	$n = 594$	$n = 621$	$n = 648$	$n = 675$	$n = 702$
Acanthocephala	239	224	130	87	3	1
Annelida	21 083	20 582	19 551	17 674	908	608
Arthropoda	2 613 568	1 860 696	1 653 239	1 432 478	54 934	44 105
Brachiopoda	7	7	6	5	1	1
Bryozoa	815	479	419	379	234	12
Chaetognatha	104	98	86	42	26	11
Chordata	239 945	234 347	224 732	203 669	59 286	39 800
Cnidaria	5 698	5 414	4 859	4 276	1 835	1 291
Cycliophora	0	0	0	0	0	0
Echinodermata	11 986	11 626	10 971	9 858	1 618	1 314
Gnathostomulida	0	0	0	0	0	0
Hemichordata	10	10	10	9	6	6
Heterokontophyta	3 827	3 798	3 763	3 731	3 553	2 380
Mollusca	53 196	49 526	44 305	33 148	5 610	3 754
Nematoda	2 411	2 314	2 127	1 513	556	471
Nemertea	548	485	452	395	49	25
Onychophora	353	227	168	56	53	52
Platyhelminthes	3 658	3 416	3 102	2 937	2 784	2 610
Porifera	1 192	832	774	618	259	153
Priapulida	3	3	3	3	1	1
Rhodophyta	20 558	20 407	20 193	19 668	4 865	4 543
Rotifera	3 606	3 119	2 594	1 796	234	219
Sipuncula	289	282	213	195	49	48
Tardigrada	553	548	522	406	175	58
Xenoturbellida	1	1	1	1	1	1

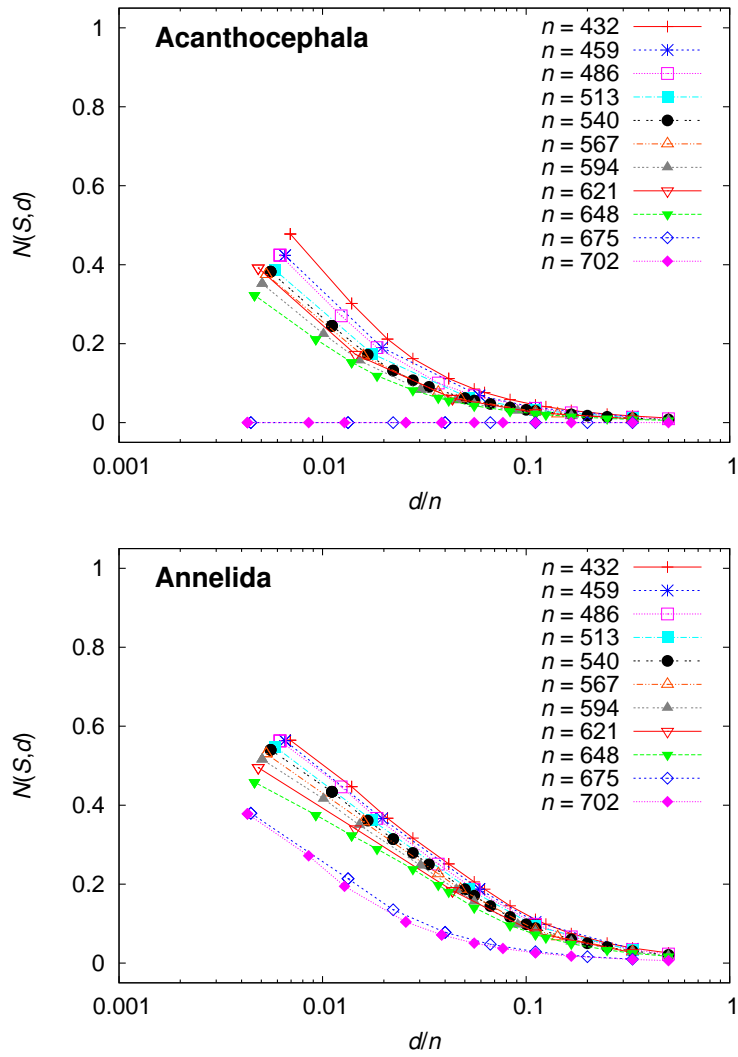


Figure A.1: The 107 $N(S, d)$ descriptors for each of the 23 phyla studied.

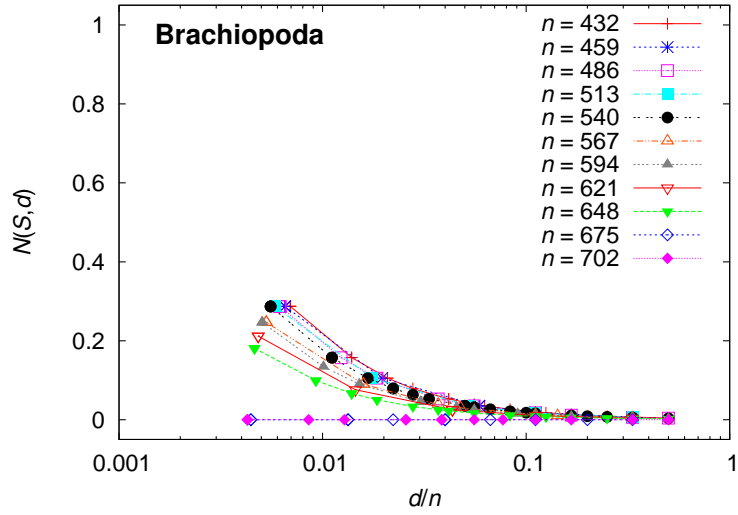
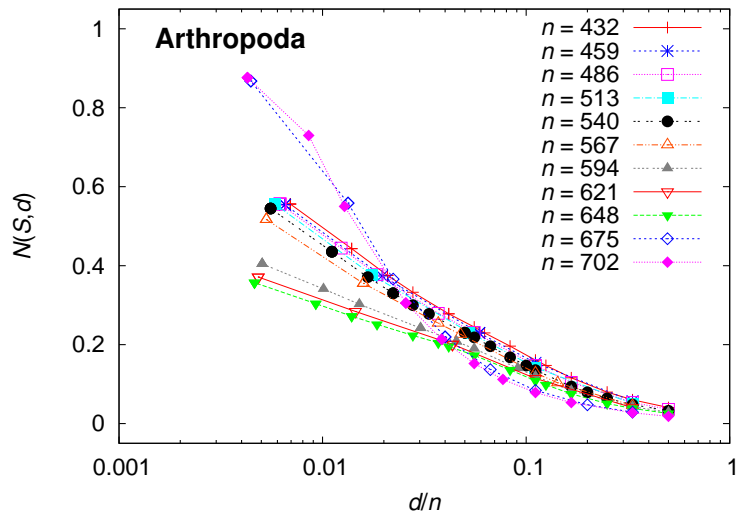


Figure A.1: Continued.

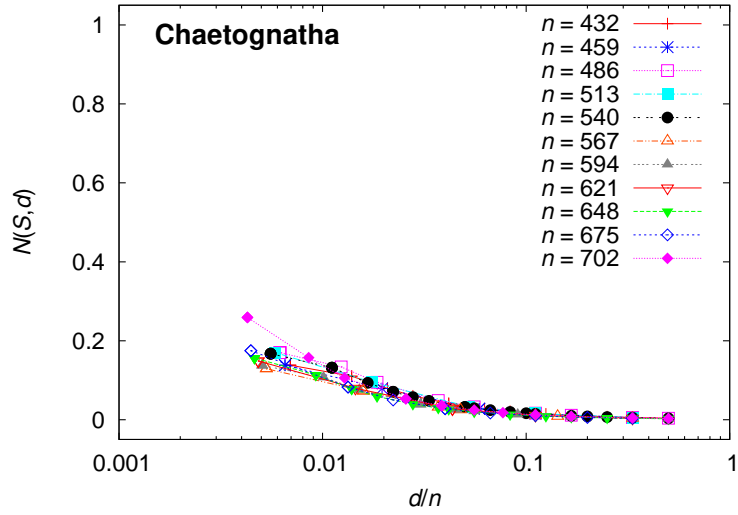
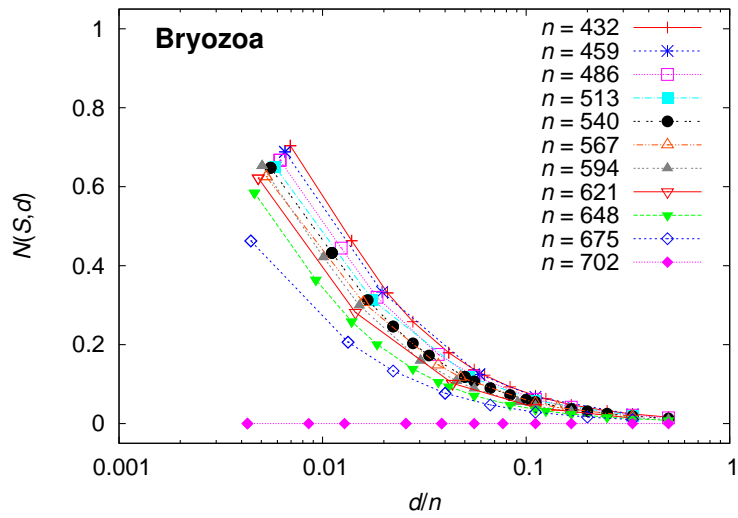


Figure A.1: Continued.

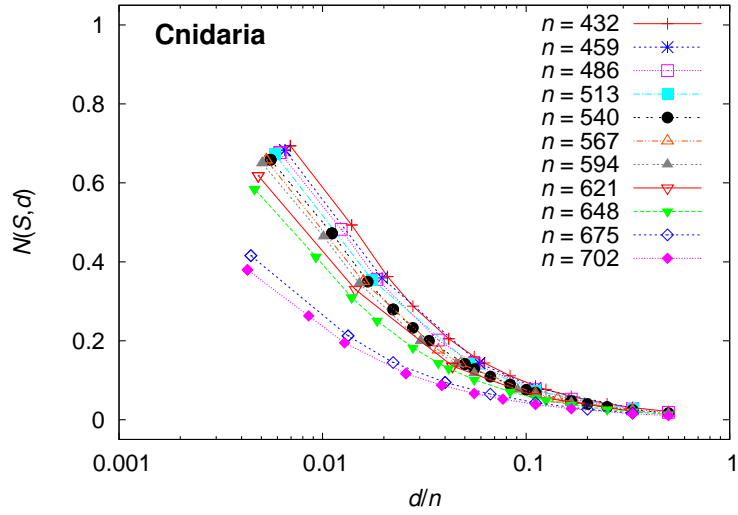
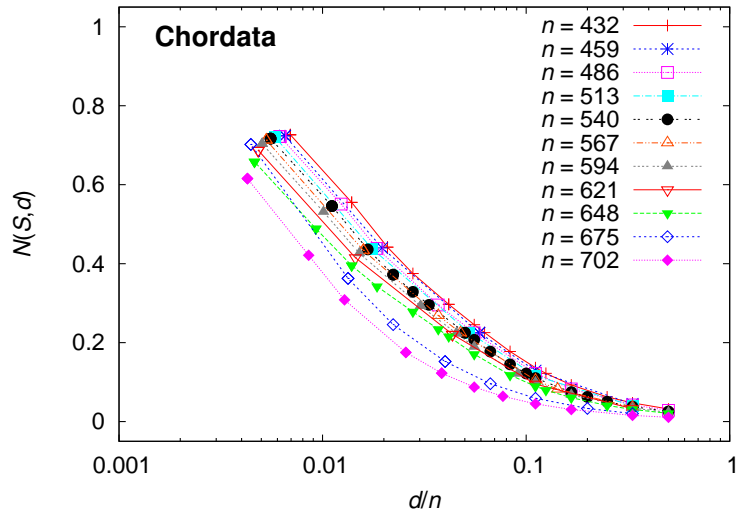


Figure A.1: Continued.

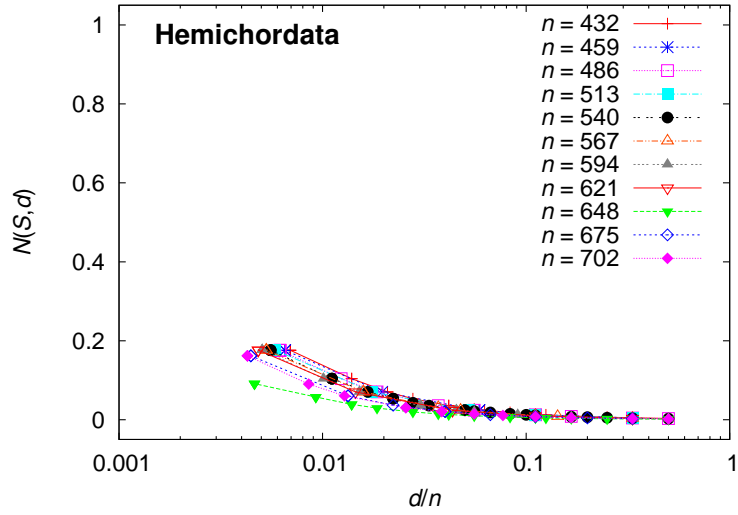
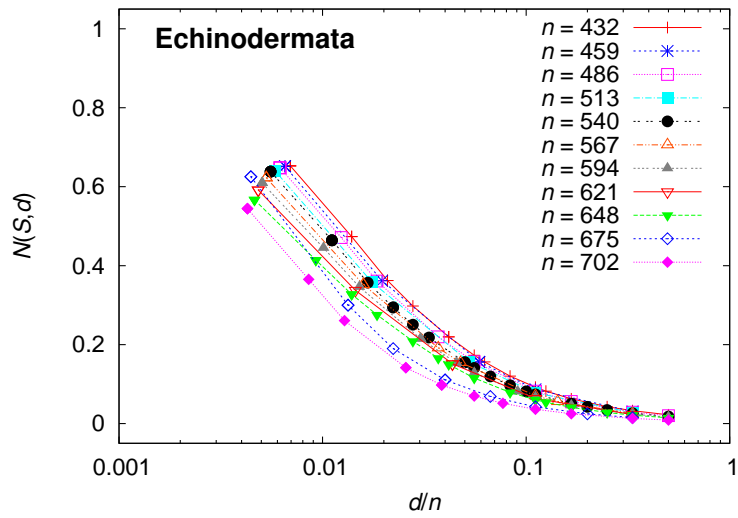


Figure A.1: Continued.

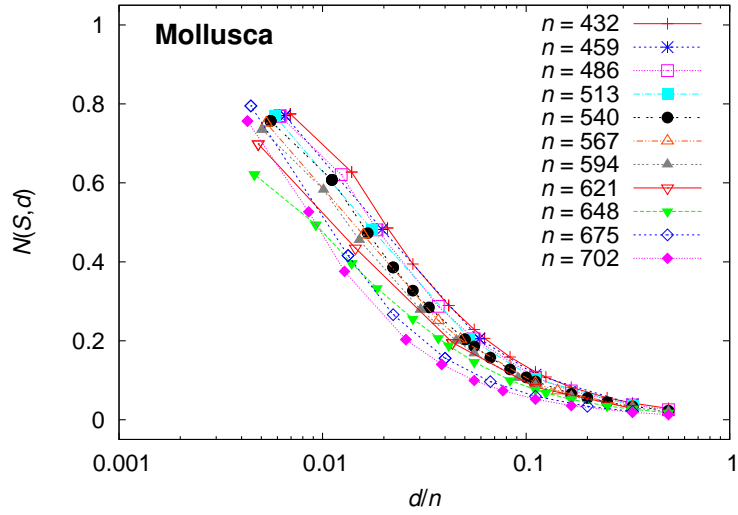
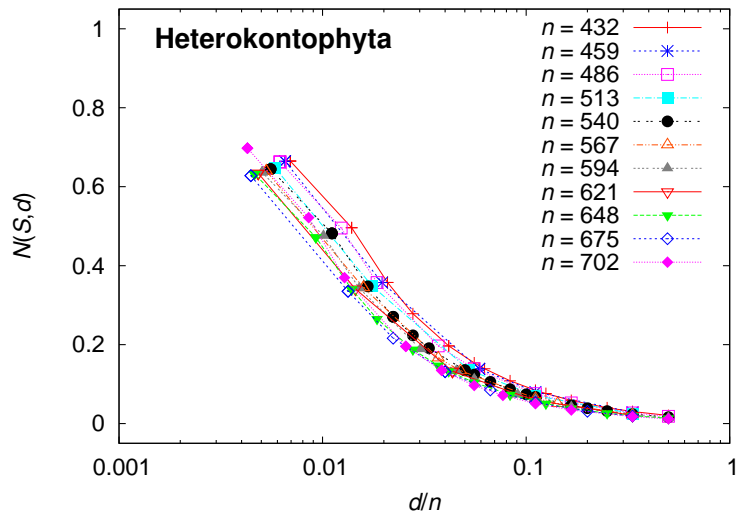


Figure A.1: Continued.

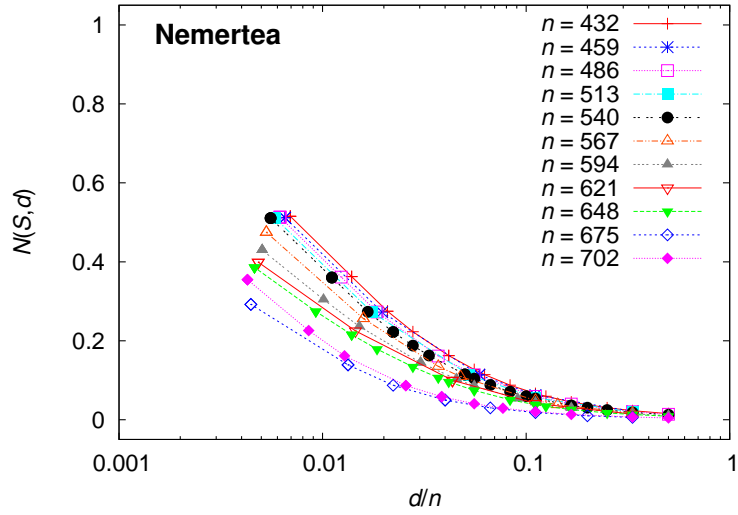
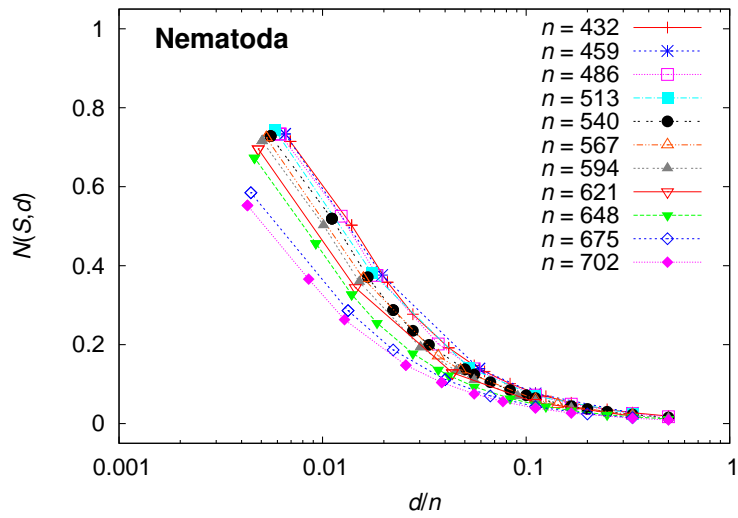


Figure A.1: Continued.

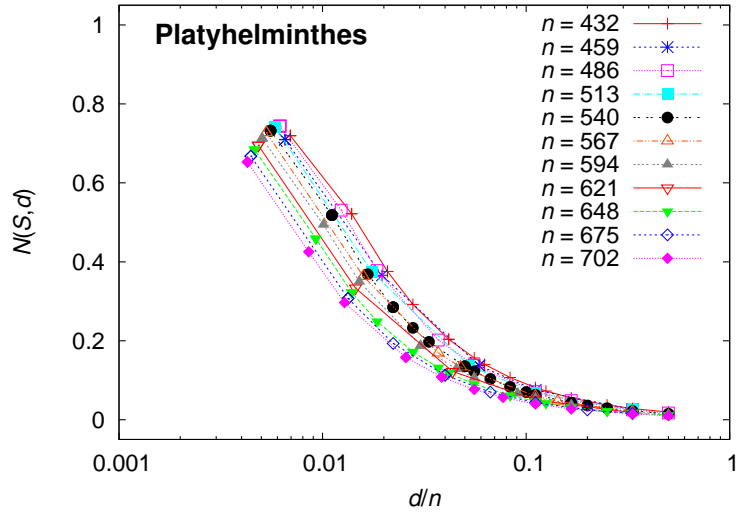
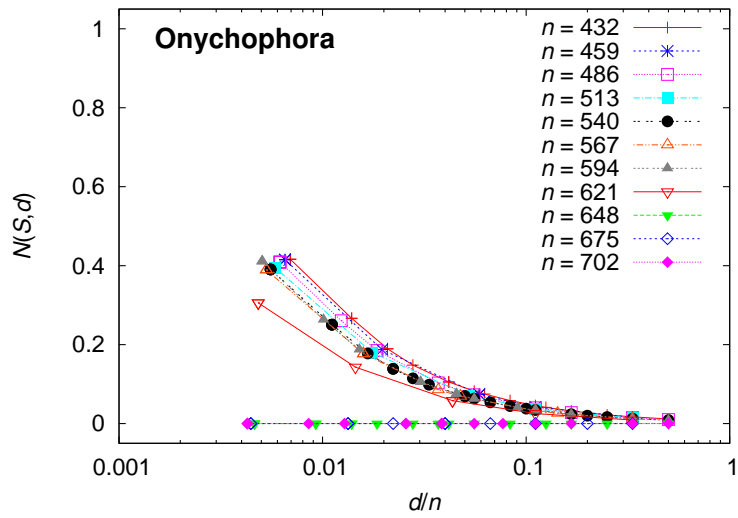


Figure A.1: Continued.

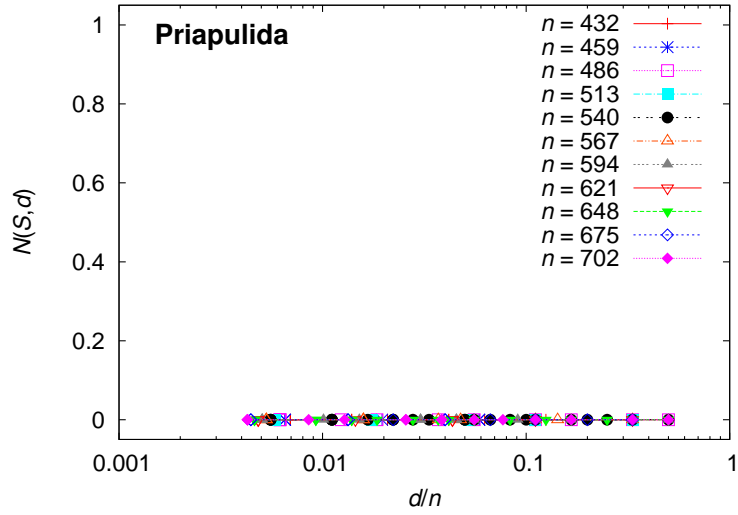
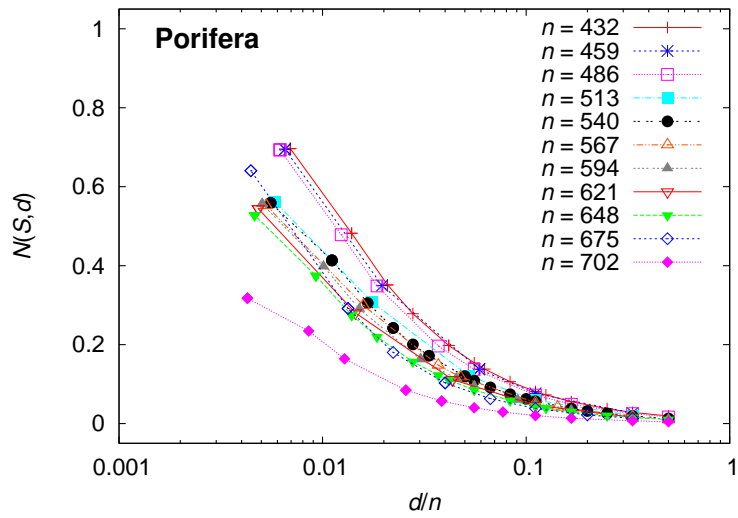


Figure A.1: Continued.

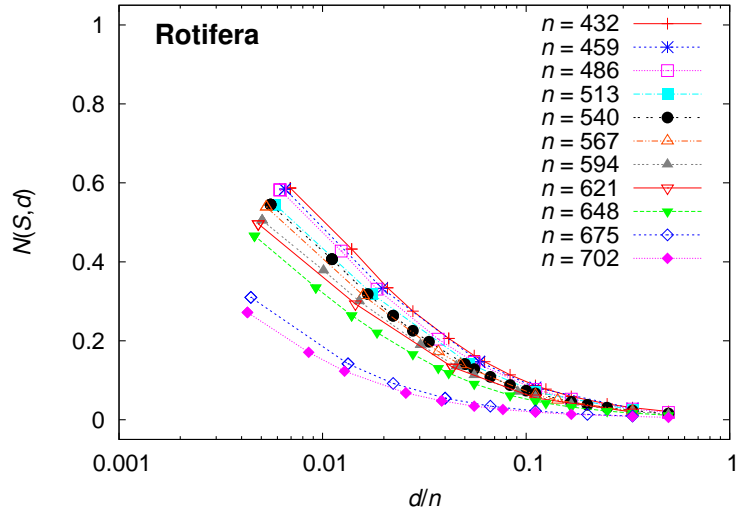
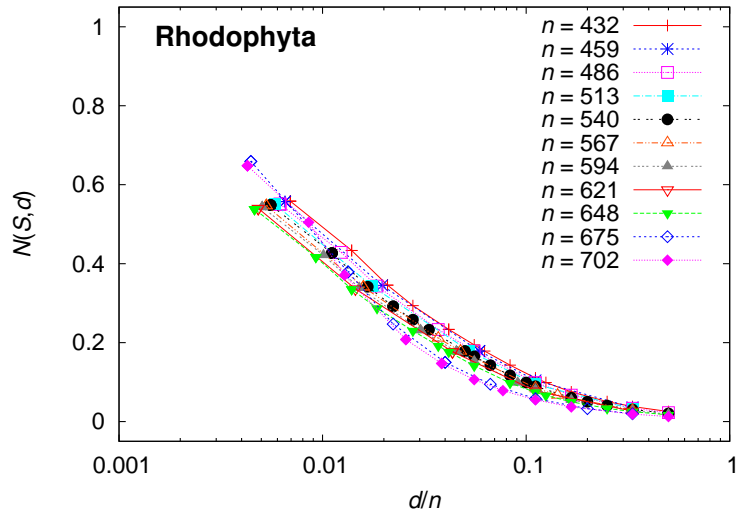


Figure A.1: Continued.

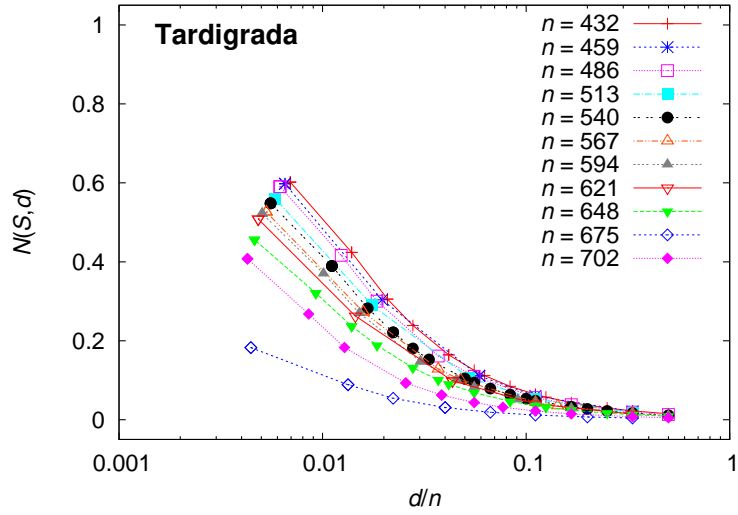
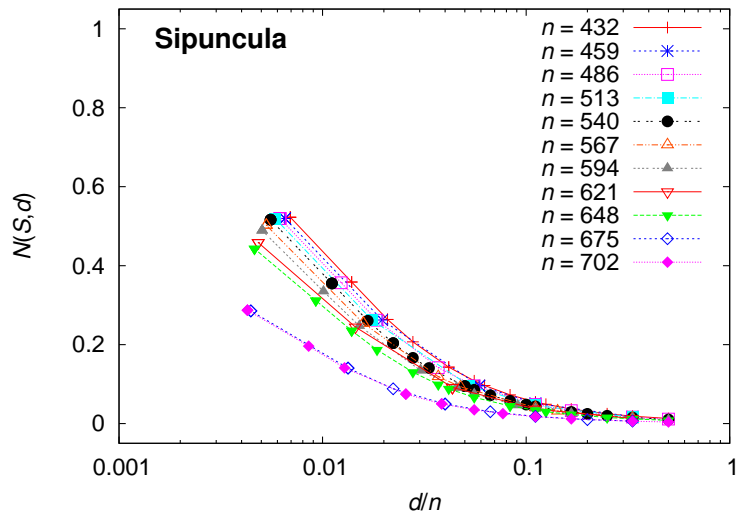


Figure A.1: Continued.

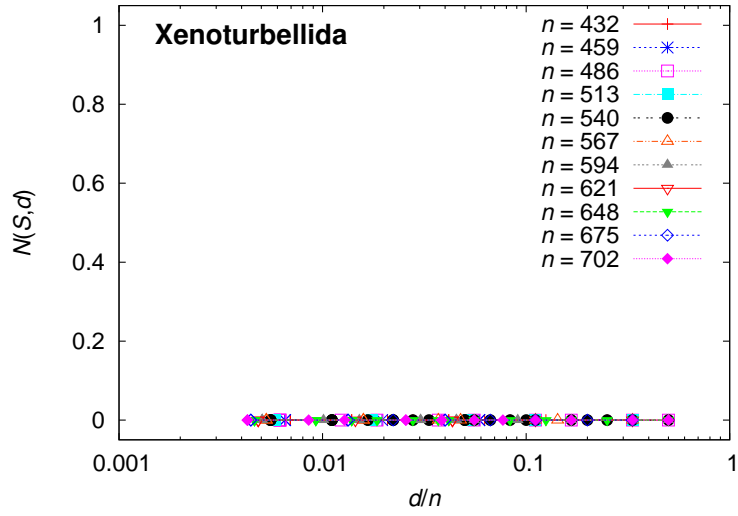


Figure A.1: Continued.

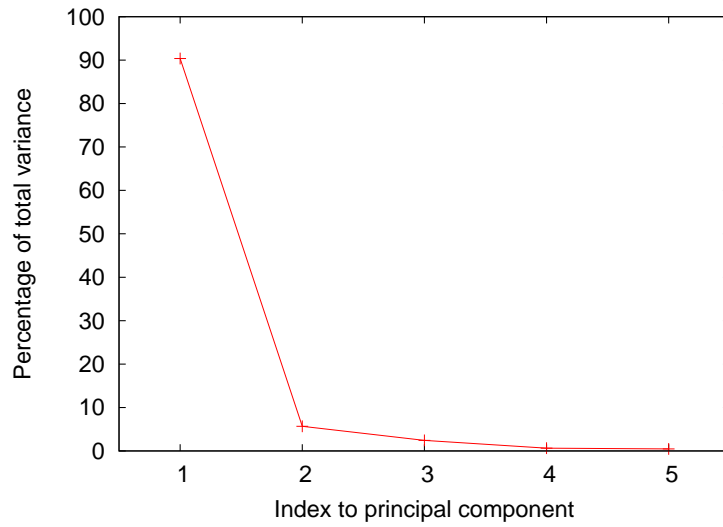


Figure A.2: Scree plot resulting from PCA on the 107 standardized $N(S, d)$ descriptors. Only the first five principal components are included.